Novel Identity and Functional Markers for Human Corneal Endothelial Cells

Alena Bartakova,[1] Karen Alvarez-Delfin,[2] Alejandra D. Weisman,[2] Enrique Salero,[2] Gabriella A. Raffa,[2] Richard M. Merkhofer Jr,[2] Noelia J. Kunzevitzky,[1–3] and Jeffrey L. Goldberg[1,2,4]

[1]Shiley Eye Institute, University of California San Diego, La Jolla, California, United States
[2]Bascom Palmer Eye Institute and Interdisciplinary Stem Cell Institute, University of Miami Miller School of Medicine, Miami, Florida, United States
[3]Emmecell, Key Biscayne, Florida, United States
[4]Byers Eye Institute at Stanford, Stanford University, Palo Alto, California, United States

Correspondence: Jeffrey L. Goldberg, Byers Eye Institute, 2452 Watson Court, Palo Alto, CA 94303-5353, USA; jlgoldbe@stanford.edu.

AB and KA-D contributed equally to the work presented here and should therefore be regarded as equivalent authors.

Submitted: December 8, 2015
Accepted: April 1, 2016

Citation: Bartakova A, Alvarez-Delfin K, Weisman AD, et al. Novel identity and functional markers for human corneal endothelial cells. *Invest Ophthalmol Vis Sci*. 2016;57:2749–2762. DOI:10.1167/iovs.15-18826

Purpose. Human corneal endothelial cell (HCEC) density decreases with age, surgical complications, or disease, leading to vision impairment. Such endothelial dysfunction is an indication for corneal transplantation, although there is a worldwide shortage of transplant-grade tissue. To overcome the current poor donor availability, here we isolate, expand, and characterize HCECs in vitro as a step toward cell therapy.

Methods. Human corneal endothelial cells were isolated from cadaveric corneas and expanded in vitro. Cell identity was evaluated based on morphology and immunocytochemistry, and gene expression analysis and flow cytometry were used to identify novel HCEC-specific markers. The functional ability of HCEC to form barriers was assessed by transendothelial electrical resistance (TEER) assays.

Results. Cultured HCECs demonstrated canonical morphology for up to four passages and later underwent endothelial-to-mesenchymal transition (EnMT). Quality of donor tissue influenced cell measures in culture including proliferation rate. Cultured HCECs expressed identity markers, and microarray analysis revealed novel endothelial-specific markers that were validated by flow cytometry. Finally, canonical HCECs expressed higher levels of CD56, which correlated with higher TEER than fibroblastic HCECs.

Conclusions. In vitro expansion of HCECs from cadaveric donor corneas yields functional cells identifiable by morphology and a panel of novel markers. Markers described correlated with function in culture, suggesting a basis for cell therapy for corneal endothelial dysfunction.

Keywords: human corneal endothelial cells, corneal endothelial dystrophy, cell therapy

The cornea is made of three cellular layers: epithelium, stroma, and endothelium. The latter is a 4-μm thick monolayer located on the inner side of the cornea responsible for maintaining corneal transparency by dehydrating the stroma. Human corneal endothelial cells (HCECs) do not regenerate in vivo to a significant degree, arresting in G1-phase of the cell cycle.[1,2] Human corneal endothelial cell density gradually decreases with age from approximately 4000/mm^2 in newborns to approximately 2300/mm^2 in the elderly,[1,3–5] and is further reduced by surgical trauma.[6–8] Additionally, HCEC survival and function are reduced in genetic diseases such as Fuchs' dystrophy.[9–12] When corneal endothelial cell density reaches a critical low, the stroma swells with edema, becomes painful, and generates a form of corneal blindness.[13–15]

Full transplant of all corneal layers (penetrating keratoplasty [PK]), and in the past decade, the selective replacement of only the damaged endothelium layer (Descemet's stripping endothelial keratoplasty [DSEK])[16] and newer variants such as Descemet membrane endothelial keratoplasty, DMEK,[17] and Descemet membrane endothelial transfer (DMET)[18,19] are the main surgical treatment options for corneal endothelial dysfunction.[20–23] However, there is a worldwide shortage of donor corneas, and complicated surgical techniques require infrastructure and access to highly trained specialists. Even in optimal conditions, the procedure is accompanied by surgical risks related to infection and inflammation, and immune rejection.[24] Therefore, along with attempts to enhance corneal endothelial function by the use of topical therapies,[25–28] a cell therapy approach based on in vitro expansion of HCECs from cadaveric corneas has been proposed as a solution.[29–33] Two fronts are being simultaneously investigated: transplant of tissue-engineered corneas, in which HCECs are seeded onto biological or synthetic scaffolds and transplanted as a sheet; and the injection of a suspension of HCECs in the anterior chamber that will attach to the host endothelium or Descemet's membrane. In order to address either approach, robust isolation methods and in vitro expansion and characterization of functional HCECs become critical.

Currently, one of the most widely used isolation techniques, a 2-step peel-and-digest nonenzymatic procedure,[34] yields reasonable HCEC numbers, but is prone to contamination by stromal keratocytes, and fibroblastic conversion, also known as endothelial-to-mesenchymal transition (EnMT), becomes evident in early passages.[34,35] Endothelial-to-mesenchymal transi-

tion results in the disruption of the cellular monolayer, loss of cell-cell contact inhibition, as well as changes in the extracellular matrix composition, cell morphology, and function.

Thus, determining potential markers that differentiate cultures with a minimum of EnMT may allow for the identification of the HCECs with highest function and selection of high-quality HCEC subpopulations to be specifically expanded for cell therapy treatment of corneal endothelial dystrophies. Here, we isolate, expand, and characterize functional HCECs in vitro as a first step towards a cell therapy.

Materials and Methods

Donor Tissue

Human cadaveric donor corneas not suitable for transplantation and preserved in Optisol-GS (Baush & Lomb, Rochester, NY, USA) were procured from the Lions Eye Institute for Transplant and Research (Tampa, FL, USA), the National Disease Research Interchange (NDRI; Philadelphia, PA, USA), Eversight (Ann Arbor, MI, USA), and the San Diego Eye Bank (San Diego, CA, USA). Donor confidentiality was maintained by the eye banks and by this laboratory according to the tenets of the Declaration of Helsinki. The age of donors ranged from 2 to 77 years, with preference for donors under 50-years old and endothelial cell counts above 2000 cells/mm^2. Corneas from donors undergoing chemotherapy at the time of death and with history of diabetes or sepsis were excluded. The time from death to preservation was on average 13 hours and primary cultures of HCECs were initiated within 14 days of preservation in Optisol-GS (Supplementary Table S1). A total of 85 corneas were used for this study.

Human Corneal Cell Culture

Primary HCECs were cultured following a previously described method.[36] Briefly, corneas were rinsed three times in M199 medium (Gibco, Rockville, MD, USA) with 50 μg/mL gentamicin (Gibco). Pieces of endothelium attached to Descemet's membrane were stripped off and stabilized overnight at 37°C in 5% CO_2 in growth medium containing: OptiMEM-I (Gibco), 8% fetal bovine serum (FBS; Hyclone, Logan, UT, USA), 5 ng/mL human recombinant endothelial growth factor (PeproTech, Rocky Hill, NJ, USA), 20 ng/mL human recombinant neural growth factor (PeproTech), 100 μg/mL bovine pituitary extract (Biomedical Technologies, Stoughton, MA, USA), 20 μg/mL L-ascorbic acid (Sigma-Aldrich Corp., St. Louis, MO, USA) or 0.5 mM L-ascorbic acid 2-phosphate (Sigma-Aldrich Corp.), 200 mg/L calcium chloride (Life Technologies, Carlsbad, CA, USA), 0.08% chondroitin sulfate (Sigma-Aldrich Corp.), 50 μg/mL gentamicin (Gibco), and 1× antibiotic/antimycotic solution (Life Technologies). The next day, the tissue was rinsed in Hanks' Balanced Salt Solution (Gibco) and incubated in 0.02% EDTA (Sigma-Aldrich Corp.) for 1 hour at 37°C. Cells were released by passing the tissue 15 to 20 times through a glass pipette and then were resuspended in growth medium. Clinical grade reagents were used whenever available. Isolated cells and remaining strips of Descemet's membrane from a single cornea were plated in a 3.8-cm^2 tissue culture plate precoated with FNC Coating Mix (Athena Environmental Sciences, Inc., Baltimore, MD, USA); this was considered passage 0 (P0). All cultures were incubated at 37°C in a 5% CO_2, humidified atmosphere. Medium was changed every other day. For each cornea, the time from plating (day 0) to next passage (80%–90% confluency) was recorded. Cell passaging was performed by digesting confluent cultures with 0.05% Trypsin (Gibco) for 5 minutes at 37°C in 5% CO_2, and cell viability was evaluated by Trypan Blue exclusion assay (Sigma-Aldrich Corp.). Corneal stromal keratocytes were isolated and cultured as described by Stramer et al.[37] Briefly, human corneas were washed twice with M199 medium with 50 μg/mL gentamicin. After the endothelium and the epithelium were removed, the central stroma was cut with an 8-mm biopsy punch (Sigma-Aldrich Corp.), and rinsed three times in PBS. Stromal discs were minced into small pieces and seeded in culture plates. Once firmly attached, cells were kept at 37°C and 10% CO_2, and fed every other day with Dulbecco's modified Eagle's medium supplemented with 10% FBS (Invitrogen) and 50 μg/mL gentamicin (Gibco). Cultures were imaged in an Axio Observer A1 phase-contrast microscope (Carl Zeiss Microscopy, GmbH, Oberkochen, Germany).

Immunohistochemistry

Human corneal endothelial cells were cultured on FNC-coated glass coverslips (Carolina Biological Supply Co., Burlington, NC, USA) placed in 24-well plates. At approximately 90% confluence, cells were fixed in 4% paraformaldehyde (Electron Microscopy Sciences, Hatfield, PA, USA) for 10 minutes and rinsed three times with PBS. Blocking and permeabilization were performed at room temperature for 30 minutes using 20% normal goat serum and 0.2% Triton X-100 in antibody buffer (150 mM NaCl, 50 mM Tris base, 1% BSA, 100 mM L-lysine, 0.04% Na azide [pH = 7.4]). Primary antibodies were diluted in antibody buffer and incubated overnight at 4°C. The primary antibodies used were: anti–ZO-1-Alexa Fluor-594-conjugated (1:100; Life Technologies) and anti-human Na^+/K^+/ATPase (1:50; Millipore, Billerica, MA, USA). After three washes in PBS, coverslips were incubated in secondary antibodies diluted 1:500 in antibody buffer for 2 hours at room temperature or at 4°C overnight, rinsed three times with PBS, mounted in Vectashield with 4′,6-diamidino-2-phenylindole (DAPI) (Vector Laboratories, Burlingame, CA, USA), and imaged using the upright fluorescent microscope Axio Imager Z1 or the confocal microscope Zeiss LSM700 (Carl Zeiss Microscopy).

Flow Cytometry

Cultured HCECs presenting canonical, fibroblastic, and mixed morphologies were trypsinized and dissociated into single cells, and counted using a Neubauer chamber. One hundred thousand cells condition were resuspended in 100 μL Opti-MEM-I without phenol red (Gibco) and 5% FBS. Cells were incubated in the dark at room temperature for 30 minutes with a combination of the following mouse anti-human monoclonal antibodies: CD56-APC, CD90-FITC, CD90-PE, CD90-Cy7, CD166-PE, CD73-FITC, and/or CD109-PE (all from BD Biosciences Pharmigen, San Jose, CA, USA), mouse anti-human CAR-PE, unconjugated mouse anti-human CD248 (Millipore), and human unconjugated Na^+/K^+ ATPase (Abcam, Cambridge, UK). A maximum of three antibodies were used per sample. All the primary antibodies were used at a 1:20 dilution. After incubating the cells with anti-CD248 or anti-α1 Na^+/K^+ ATPase, they were stained with 5% Brilliant Violet 421 goat anti-mouse IgG secondary antibody (BioLegend, San Diego, CA, USA) for 15 minutes in the dark. Flow cytometric data was acquired using a BD Facs Canto flow cytometer and FACSDiva software (BD Biosciences, San Jose, CA). For each run, voltages were adjusted using an unstained HCEC control sample and single color positive controls (anti-mouse beads, stained with one single antibody: AbC Anti-Mouse Bead Kit; Invitrogen). Computer compensation was applied during data acquisition. Data was stored in a FCS file format, and further analysis was performed using FlowJo V X.0.7 (FlowJo LLC, Ashland, OR,

Investigative Ophthalmology & Visual Science

USA). Briefly, a viable HCEC population was isolated by gating on the FSC-A versus SSC-A dot plot (population 1). Doublets were excluded by performing two consecutive additional gatings (FSC-A versus FSC-W, "population 2" and SSC-A versus SSC-W, "population 3"). To quantify the expression of each marker, population three of each sample was used to create a fluorescence histogram. An overlay of the positive histogram and the negative control histogram was created for each fluorophore. Three gates including 0.1%, 1%, or 10% of the negative population were selected, and the percentage of positive cells present in these gates was assessed. The threshold of 1% best highlighted the changes of marker expression between canonical, mixed, and fibroblastic cell populations, and therefore was selected for subsequent analysis. Given the similarity of unstained canonical and fibroblastic HCECs when analyzed by flow cytometry, either canonical or fibroblastic HCECs were used as negative controls for each run.

To compare the expression of CD56 to other markers (CD109, CD248, and CAR), a quadrant dot plot was created, using the negative control population three to determine the limits of the four quadrants. The percentage of cells inside each quadrant was quantified as labeled in each graph.

RNA Isolation

Cultured HCECs in passage 0 and whole donor corneas were used for RNA extraction. Fresh donor corneas stored in Optisol-GS (Baush & Lomb, Rochester, NY, USA) were minimally processed and the epithelial, stromal, and endothelial layers were isolated. Ribonucleic acid extraction from donor corneas and cultured HCECs was performed using the RNEasy Kit (HCECs, endothelium, and epithelium; manufacturer's protocol; Qiagen, Valencia, CA) or Trizol (stroma[38]). Purified RNA was quantified and analyzed with a Nanodrop spectrophotometer (Thermo Scientific, Wilmington, DE, USA). Ribonucleic acid samples were stored at –80°C until used.

Transendothelial Electrical Resistance (TEER)

Per transwell, 20,000 cells were seeded in 24-well plates (6.5-mm diameter, 0.4-μm pore; Costar, Corning, NY, USA), previously coated with FNC. Transendothelial electrical resistance was measured with an EVOM2 epithelial volt-ohmmeter (World Precision Instruments, Sarasota, FL, USA) for 30 days or until readings reached a steady state, whichever happened first. Transendothelial electrical resistance measurements were normalized to the value of the control wells (growth media without cells). The reported values represent the average reading of at least three wells per condition. A bovine corneal endothelial cell line (BCEC) was used as a positive control (ATCC CRL-2048, Manassas, VA, USA) and fibroblastic HCECs were used as a negative control.

Microarray Analysis

Ribonucleic acid from at least three biological replicates was independently collected as described above and its quality was assessed with NanoDrop (Thermo Scientific) and confirmed with RIN (RNA integrity number) at the University of Miami Center for Genome Technology (Miami, FL, USA). Amplification and processing for hybridization to GeneChip Human Gene ST 1.0 arrays (Affymetrix, Santa Clara, CA, USA) were performed at the University of Miami Center for Genome Technology (Miami, FL, USA) following standard protocols. Data were normalized with Genespring 12.0 (Agilent, Santa Clara, CA, USA) and filtered by intensity. Probes between the 20th and 99th percentile range in at least two of three samples per condition were included in the analysis. Statistical comparison between conditions was performed using unpaired Student's *t*-test with Benjamini-Hochberg correction for multiple testing. Final data analysis was conducted using Excel software (Microsoft Corporation, Redmond, WA, USA) and GeneGo (Thomson Reuters, Philadelphia, PA, USA).

Statistical Analysis

Data are expressed as mean ± SEM unless noted otherwise. Statistical analysis was performed using unpaired, 2-tailed Student's *t*-test; P less than 0.05 was considered statistically significant.

Results

Isolation and In Vitro Expansion of HCECs

We first asked whether HCECs in vitro maintain the characteristics observed in vivo, namely cell–cell contact inhibition and the canonical cobblestone-like or polygonal morphology. Corneal endothelial cells were isolated and cultured from cadaveric donor corneas following a previously published method[36] outlined in Figure 1A. Cells cultured at high density and for a lower number of passages often formed a monolayer with polygonal "canonical" morphology (Figs. 1B–E). Typically, the canonical morphology was maintained until passage three or four, similar to previous observations.[29,39] At later passages, cells often underwent EnMT, exhibiting fibroblastic morphology, and losing cell–cell contact inhibition (Fig. 1F). An exceptional culture from a 15-year-old donor was cultured up to passage 10 without signs of fibroblastic conversion, but at passage 12, senescence was evident (Fig. 1G) as cells became enlarged and proliferation rate dramatically decreased (not shown). Overall, HCECs from younger corneas, cultured in vitro, were expanded for 3 or 4 passages, with each cornea yielding a variable number of total cell progeny (Fig. 1H) that may be adequate to treat several patients.

We asked whether the age of the donor influenced culture quality, as has been previously suggested.[34] We looked at the time to reach confluency from passage 0 (P0) to passage 1 (P1) and found that corneas from younger donors (2- to 34-years old) took, on average, 11 days to become confluent, whereas corneas from older donors (38- to 77-years old) took 19 days (Fig. 1I). We also found a weak but significant correlation between initial endothelial cell density and time to confluency (Fig. 1J). Finally, there was a significant difference in initial endothelial cell density between corneas from young donors (2- to 34-years old: average endothelial cell density: 3181.6 mm^2; range, 2571–4425 mm^2; $n = 30$) and those from older donors (38- to 77-years old: average endothelial cell density: 2761.5 mm^2; range 1969–2865 mm^2; $n = 11$). Tissue from younger donors had significantly higher endothelial cell counts compared with older donors ($P = 0.02$; Fig. 1K). We generally observed that cultures from younger donors demonstrated better attachment and a more uniform morphology. However, cultures from young donors with sepsis or undergoing chemotherapy were not successful, suggesting a direct relationship between HCEC culture outcome and donor age and health.

Identity and Function of HCECs In Vitro

There is a paucity of HCEC-specific identity markers, and the expression of proteins expressed ubiquitously in tight junction complexes is often cited for identity criteria.[40,41] For example, we found cultured HCECs expressed such markers including

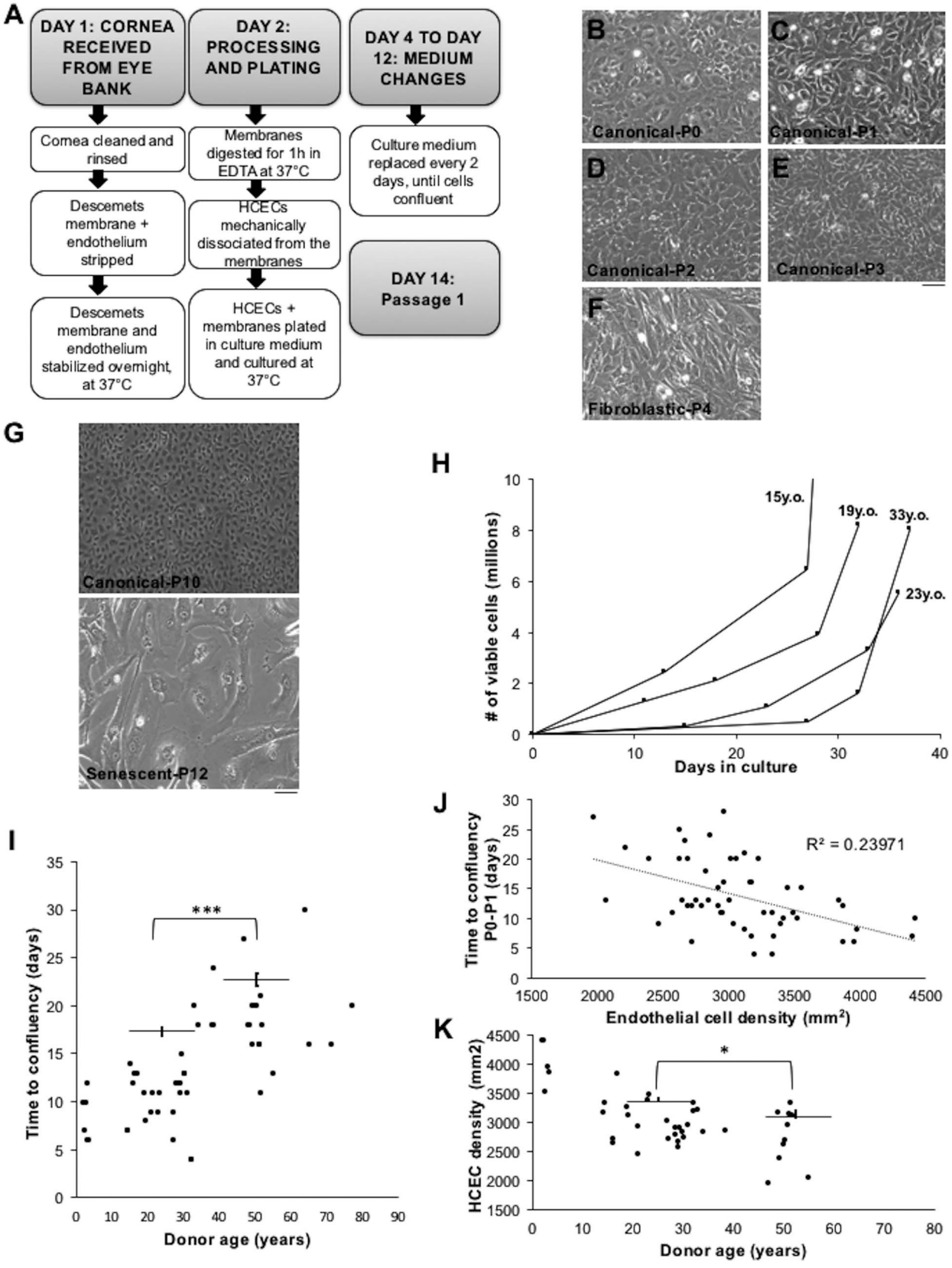

Figure 1. Human corneal endothelial cells isolation and culture. (**A**) Outline of the HCEC isolation and primary culture. (**B–G**) Bright-field micrographs of cultured HCECs at different passage (P) numbers. Primary cultures of HCECs often demonstrated the distinctive cobblestone-like morphology until P3 or P4 (**B–E**); at later passages (**F**) fibroblastic conversion was common. (**G**) An exceptional culture maintained canonical morphology to P10, but by P12 showed senescent characteristics including lengthened cells and slowed growth rate. *Scale bars*: 50 μm. (**H**) Cell yields after expansion of HCECs from corneas of young donors for three or four passages. (**I**) Scatter plot of the time to confluency in relation to donor age: HCECs cultured from younger donors (average age: 22 years old; range, 0–34 years; $n = 35$) showed significantly greater proliferation

rates (***$P < 0.0001$) compared with older donors (average age: 50 years old; range, 35–77 years; $n = 20$). (**J**) There is a weak correlation between HCEC density and in vitro proliferation ($r^2 = 24\%$), but the correlation is statistically significant ($P = 0.0002$). (**K**) There was a statistically significant difference between corneal endothelial density measured before enucleation in younger donors (average endothelial cell density: 3181.6 mm^2; range, 2571–4425 mm^2; $n = 30$) compared with older donors (average endothelial cell density: 2761.5 mm^2; range, 1969–2865 mm^2; $n = 11$; $P = 0.02$).

the tight junction protein ZO-1 and the channel Na^+/K^+-ATPase. Human corneal endothelial cells in culture, morphologically similar to cells represented in Figures 1B to 1E, immunostained for ZO-1 exhibited typical honeycomb staining at the tight junctions, while Na^+/K^+-ATPase expression was found basolaterally (Fig. 2A), but Na^+/K^+-ATPase was also expressed by HCECs with fibroblastic morphology (Fig. 2B), thus failing to identify canonical HCECs specifically. We also examined the barrier function of the HCEC monolayer using a TEER assay, where higher resistance values indicate less permeability at intercellular junctions and therefore, better function. We hypothesized that cells undergoing EnMT and demonstrating fibroblastic morphology would have lower barrier function. We found that cultures with the canonical cobblestone-like morphology reached significantly higher TEER values than fibroblastic cultures, and cultures with mixed morphology of fibroblastic and hexagonal cells demonstrated intermediate values of TEER (Fig. 2C). Thus, HCECs can be identified by the expression of a combination of markers, and their function can be determined by TEER, but the markers used routinely may not have the ability to differentiate canonical HCECs from fibroblastic HCECs or stromal fibroblasts

Canonical HCECs Express a Subset of Specific Markers That Define Their Identity

Because the routinely used markers such as ZO-1[42] appear insufficient to distinguish between canonical and fibroblastic HCECs, (Fig. 2), and identifying specific markers for HCECs with the highest barrier function remains a major interest, we next tried to find surface markers to discern between these cell phenotypes. We performed a microarray analysis comparing the transcriptomes of freshly dissected corneal layers (epithelium, stroma, and endothelium) and of P0-cultured HCECs, and found that of 28,869 probes, 23,286 (81%) were expressed by at least two of three replicates within at least one condition. Ignoring level of expression, many genes were expressed by multiple tissues but some were expressed by subsets or uniquely in single tissues or cells (Fig. 3A). Principal component analysis revealed four distinct clusters that matched the different tissue samples (Fig. 3B). There was very little intersample variability, with Pearson's correlation (r^2) greater than 0.94 (Fig. 3C). Using hierarchical clustering we found that cultured HCECs were more similar to endothelium than to stroma and epithelium (Fig. 3D). Thus transcriptomic analysis points to the consistency of cell types in vitro and to the similarity between HCECs in vivo and in vitro.

We subsequently focused our analysis on a subset of surface markers with high expression in the endothelium (P0-HCECs and freshly dissected tissue) but low expression in stroma, and that did not differ significantly between cultured or fresh endothelium (Table). To address whether the expression of such markers in HCECs was affected by fibroblastic EnMT, HCEC cultures demonstrating canonical, mixed and fibroblastic morphologies (Figs. 5A–C) were assessed for expression of the surface proteins CD56, CAR, CD248, and CD109 by flow cytometry. In a series of independent experiments, we observed a significant difference between canonical and fibroblastic cells in the expression of CD56, CAR, CD248, and CD109 surface markers (Figs. 5D–G). Whereas 97% of canonical HCECs were positive for CD56, 92% for CD248, and 82% were positive for CAR, these markers decreased as the cells lost their canonical morphology and became fibroblastic. Conversely, CD109 expression was less often detected in canonical HCECs (26% on average), and increased in expression when the cells underwent EnMT to 52% in fibroblastic cell cultures. Quadrant dot plots of canonical and fibroblastic cultures (Figs. 6A–F) revealed that canonical HCECs were mostly $CD56^{Hi}/CD248^{Hi}/CAR^{Hi}/CD109^{Lo}$. Thus, this series of markers detects shifts in cultured human HCECs from canonical to fibroblastic morphology.

Recently other groups reported the expression of CD73, CD166, CD9, and CD90 in corneal endothelial cells.[43,44] We analyzed by flow cytometry canonical and fibroblastic HCECs in passages two to three and five through eight, respectively, and the high expression of those markers did not vary with morphology (Fig. 6G). Thus, while these markers may be used to identify HCECs, they may not be adequate to select cell phenotypes based on morphology or function.

Finally, we examined whether marker expression predicted functional capacity in an in vitro TEER assay. We used confluent HCECs that we plated for TEER, isolating a subset to be tested by flow cytometry for CD56 expression. Cells exhibiting a canonical morphology and a $CD56^{high}$ marker expression demonstrated a superior barrier formation ability measured by TEER, compared with morphologically mixed or fibroblastic, $CD56^{low}$ cells (Fig. 6H). Thus, surface makers

Table. Top 10 HCEC Surface Markers

Affy Probe ID	Gene Symbol	Gene Name	Fold Change, HCECs/Endothelium	Fold Change, HCECs/Stroma
7907160	*ATP1B1*	ATPase, Na^+/K^+ transporting, beta 1 polypeptide	−2.09	6.99
7949588	*CD248*	Endosialin	1.12	5.39
7985522	*ADAMTSL3*	ADAMTS-like 3	1.12	3.88
8150537	*SLC20A2*	Solute carrier family 20 (phosphate transporter), member 2	−1.07	3.87
8142194	*LAMB1*	Laminin, beta 1	−1.22	3.79
8011747	*SLC25A11*	Solute carrier family 25 (mitochondrial carrier; oxoglutarate carrier), member 11	−1.07	3.08
8081431	*ALCAM*	Activated leukocyte cell adhesion molecule, CD166	−1.06	2.66
7904254	*ATP1A1*	ATPase, Na^+/K^+ transporting, alpha 1 polypeptide	−1.25	2.31
8081657	*CD200*	OX-2 membrane glycoprotein	−1.73	2.13
7943892	*NCAM1*	Neural cell adhesion molecule 1, CD56	−1.99	1.26

Investigative Ophthalmology & Visual Science

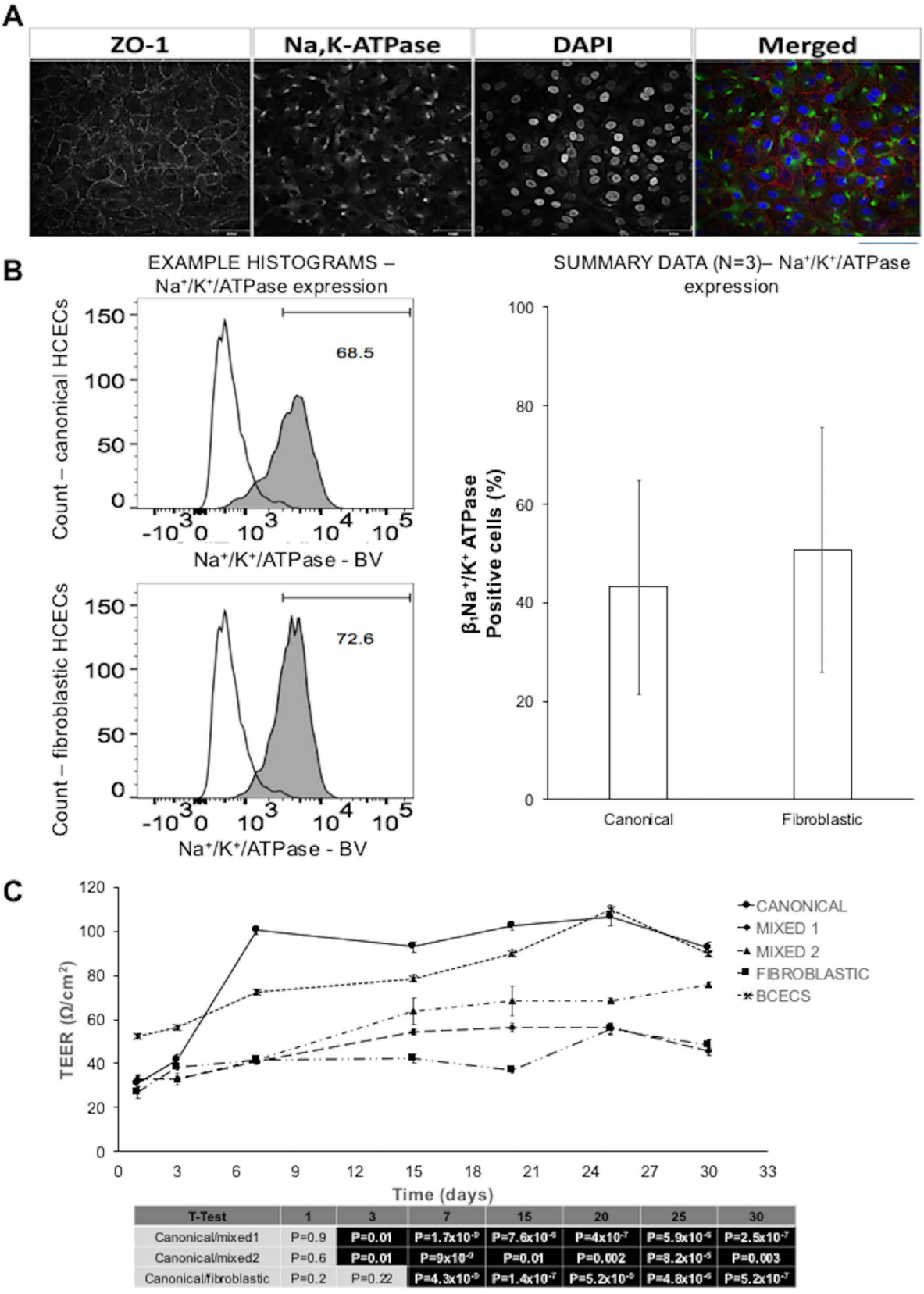

T-Test	1	3	7	15	20	25	30
Canonical/mixed1	P=0.9	P=0.01	$P=1.7\times10^{-5}$	$P=7.6\times10^{-6}$	$P=4\times10^{-7}$	$P=5.9\times10^{-6}$	$P=2.5\times10^{-7}$
Canonical/mixed2	P=0.6	P=0.01	$P=9\times10^{-9}$	P=0.01	P=0.002	$P=8.2\times10^{-5}$	P=0.003
Canonical/fibroblastic	P=0.2	P=0.22	$P=4.3\times10^{-9}$	$P=1.4\times10^{-7}$	$P=5.2\times10^{-9}$	$P=4.8\times10^{-6}$	$P=5.2\times10^{-7}$

Figure 2. Cultured HCECs express characteristic tight-junction-associated markers. (**A**) Confocal micrographs of cultured HCECs immunostained for ZO-1 and Na/K-ATPase; nuclei were counter-stained with DAPI. *Scale bar*: 50 μm. (**B**) *Bar graph* showing no difference between canonical and fibroblastic HCECs in Na/K-ATPase expression by flow cytometry ($N = 3$). Histograms of one representative flow cytometry run show no difference in Na/K-ATPase expression between canonical and fibroblastic cells. (**C**) Human corneal endothelial cells function assessed by TEER measurements from different HCEC cultures. A bovine corneal endothelial cell line (BCEC-line) was used as positive control ($N = 4$). *P* values resulting from the statistical analysis of TEER measured on canonical HCECs compared with mixed 1, mixed 2, and fibroblastic HCECs are presented in the Table below the *graph*.

Investigative Ophthalmology & Visual Science

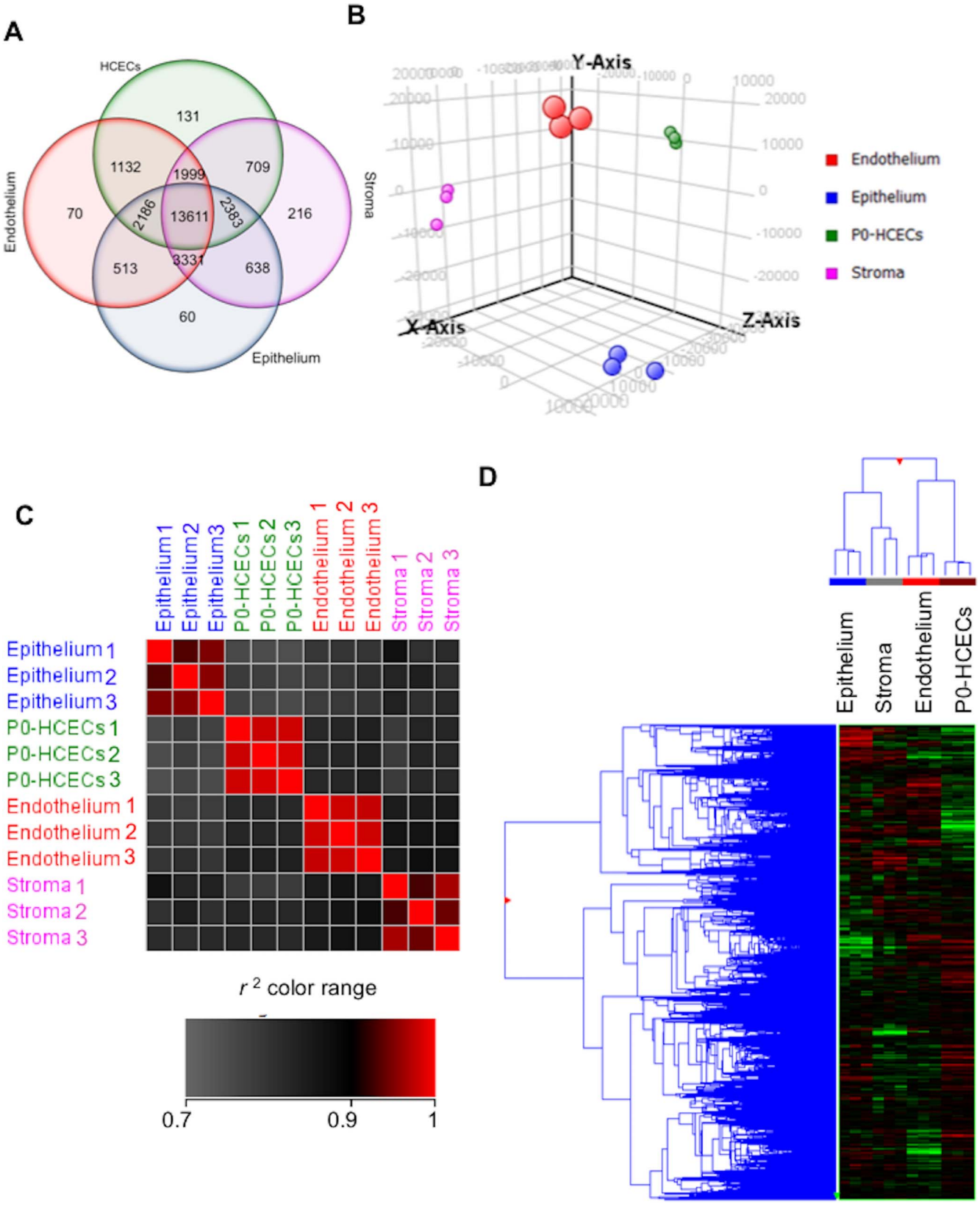

Figure 3. Transcriptome analysis of corneal layers and cultured HCECs. (**A**) *Venn diagram* representing the probes expressed in the microarray dataset in the three corneal layers and freshly cultured HCECs. (**B**) Principal component analysis revealed distinct clusters per sample type as labeled; biological replicates (*dots* with the same color) clustered together. (**C**) Pearson correlation (r^2) was higher within biological replicates than across different tissues ($N = 3$). (**D**) Hierarchical clustering demonstrated that HCECs and endothelium were more closely related than epithelium and stroma.

Investigative Ophthalmology & Visual Science

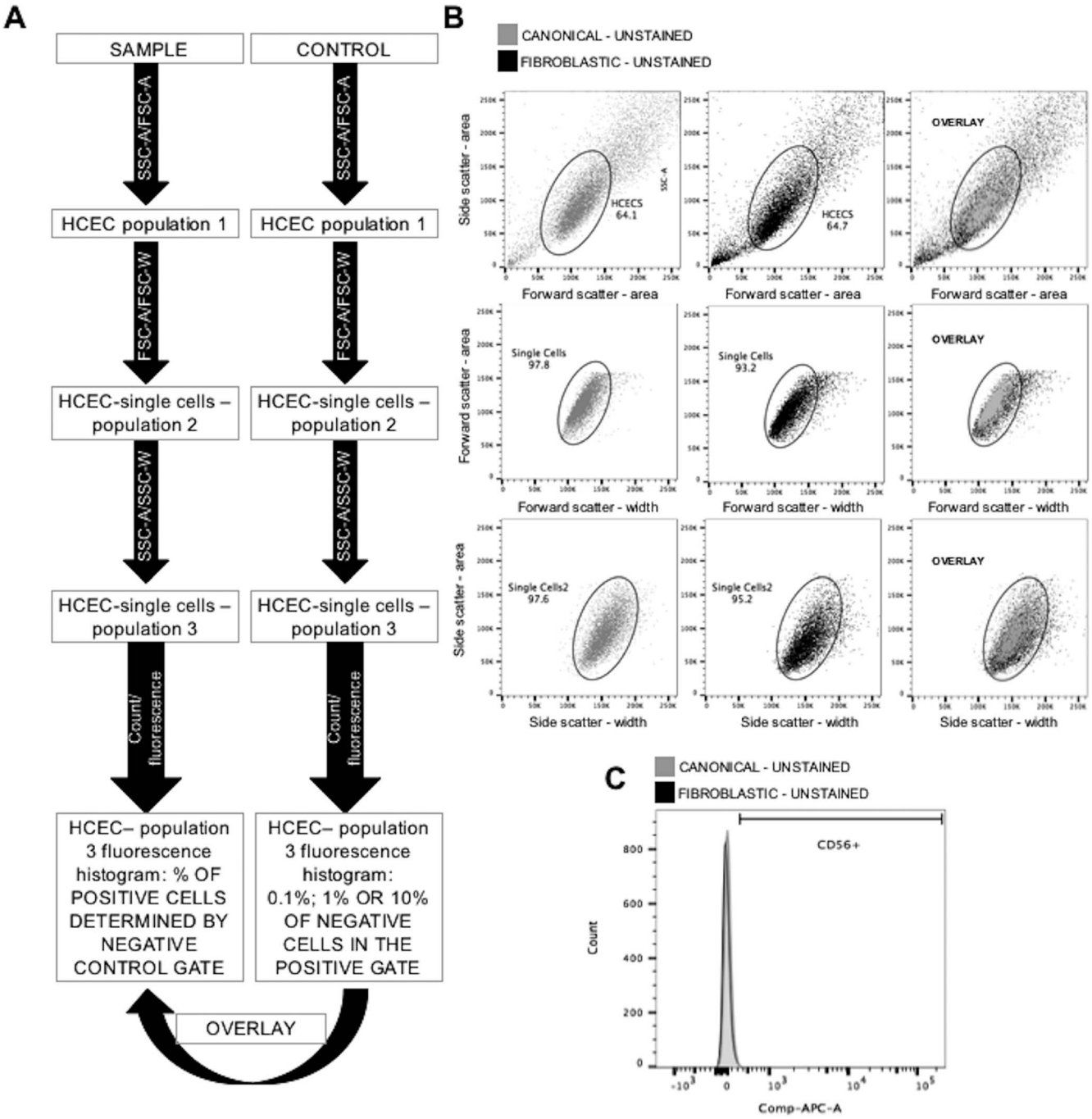

Figure 4. (A) Graphical outline of the gating process. (B) Representative 2D dot plots showing no difference in size and internal complexity between unstained canonical and unstained fibroblastic HCECs. (C) Representative histogram showing no difference in baseline fluorescence between unstained canonical and fibroblastic HCECs.

together with morphology can be used to characterize a functionally superior HCEC culture.

Discussion

Corneal endothelial insufficiency is currently treated by different variants of corneal transplant, replacing either the whole cornea or the endothelial layer. These are limited by tissue availability, access to highly trained specialists, surgical complications, immune rejection, and cost. Here we describe steps toward corneal endothelial cell therapy based on in vitro culture, expansion and identification of high quality, functional HCECs.[45] A successful culture starts with good quality donor tissue: the origin and qualities of the donor cornea including donor age, health status, and use of chemotherapy or other toxic substances play a large part in proliferative potential, morphology, and function.[34,46,47] Here, we also documented the positive correlation between younger donor age and proliferation and total cell yield.

With increasing numbers of passages in culture, EnMT often occurs and the HCECs lose their canonical cobblestone morphology and functional efficacy in barrier formation, in

Investigative Ophthalmology & Visual Science

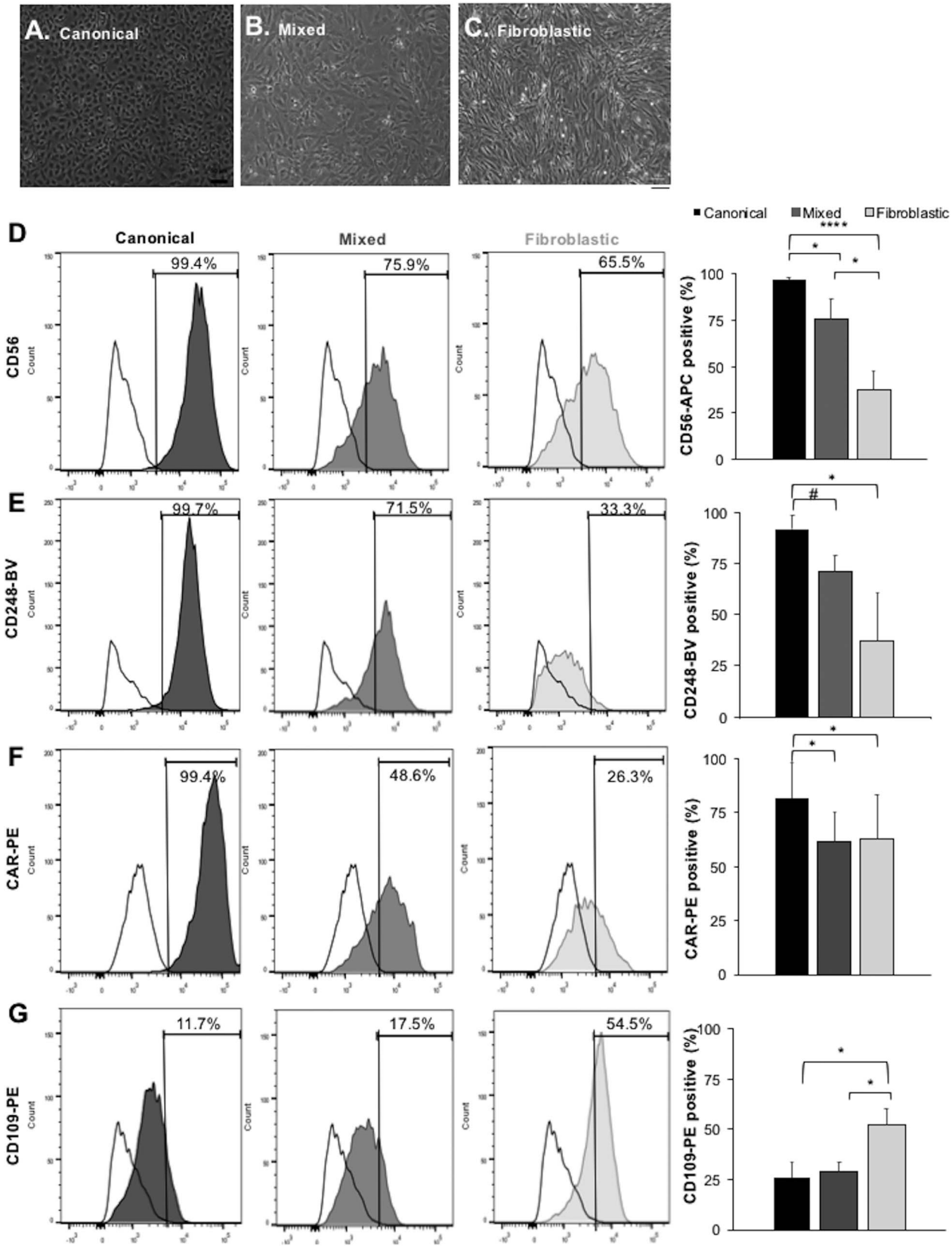

Figure 5. Flow cytometry analysis of surface markers expression differentiates HCEC subpopulations in culture. (**A–C**) Three morphologically distinct HCEC cultures, canonical, mixed, and fibroblastic as marked, were carried forward for flow cytometry. (**D–G**) Surface marker expression by flow cytometry. Flow cytometry histograms are representative illustrations of each antibody expression profile. For quantification, a threshold at the top 1% of negative control cells was set to identify positive cells throughout all the independent experiments. Quantification of the percentage of positive cells for each marker showed that CD56 (**D**), CD248 (**E**), and CAR (**F**) expressions are low in a fibroblastic culture, while CD109 (**G**) is high. Data is representative of three or more independent experiments from separate corneal cultures (CD56: $N = 10$; CD109: $N = 6$; CD248: $N = 3$; CAR: $N = 4$; P values: #0.1; *<0.05; **<0.001; ***<0.0001).

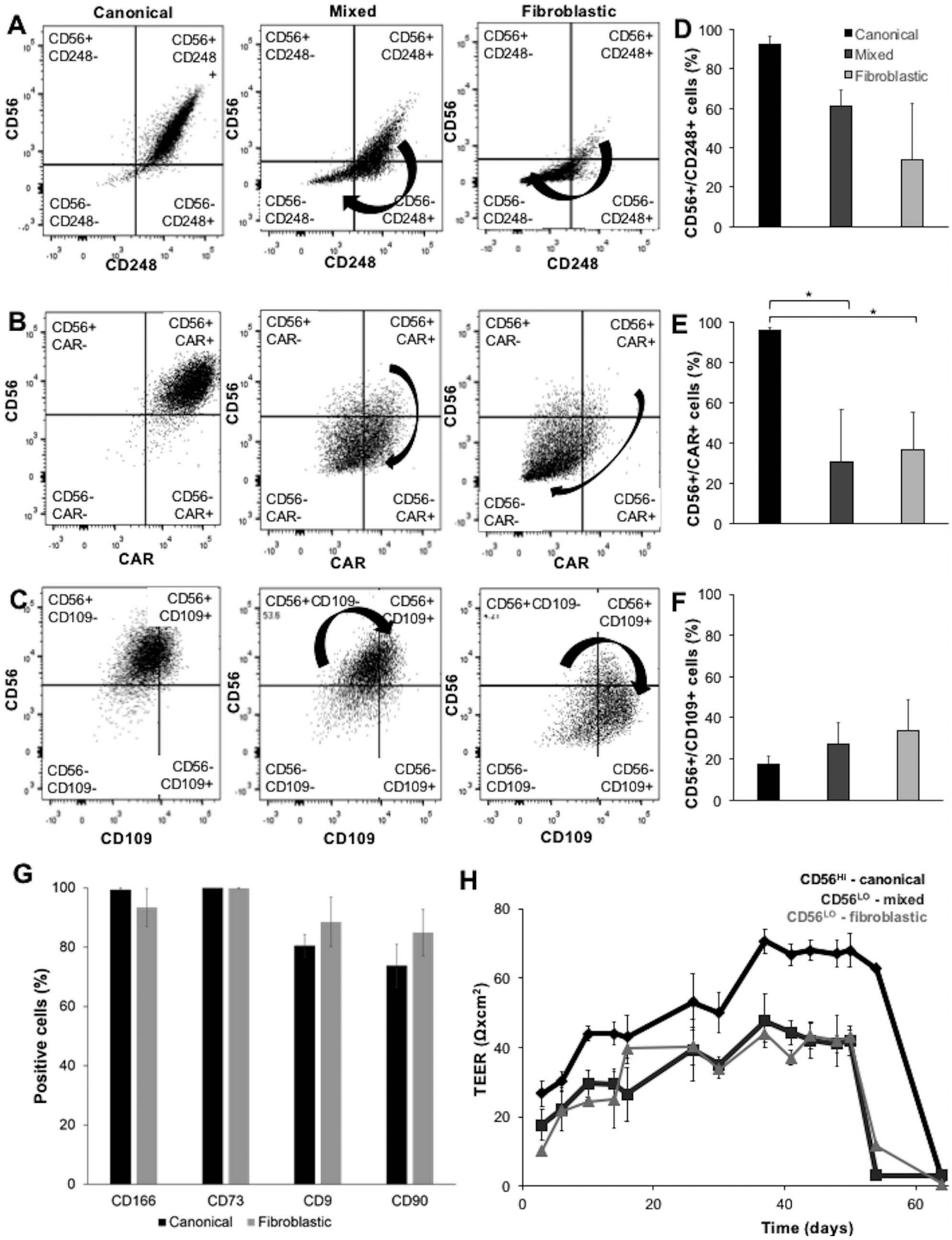

Figure 6. (**A–C**) Flow cytometry analysis by dual-color fluorescent dot plot histograms for the canonical (**A**), mixed (**B**), and fibroblastic (**C**) HCEC cultures show shift in the expression of CD56, CD248, CAR, and CD109 surface markers. Each *graph* is divided into *four quadrants* determined by the autofluorescence of unstained control cells as in Figure 4, and gated to include 99% of unstained cells in the lower left quadrant (all negative markers). (**D–F**) Quantification of the percentage of canonical, fibroblastic, and mixed cell populations expressing markers tested in pairs, as marked. (**G**) Quantification of flow cytometry experiments showing no difference between canonical and fibroblastic cells in CD166/ALCAM, CD73, CD9, CD90, and $\beta_1 Na^+/K^+$ ATPase expression. (**H**) Transendothelial electrical resistance assay using in vitro expanded HCECs whose CD56 expression had been determined by flow cytometry, demonstrating the greater ability of canonical $CD56^{high}$ cells than fibroblastic $CD56^{low}$ to form a barrier.

vitro and in vivo.[31,48] Molecular and cellular mechanisms are not yet completely understood, but inflammatory molecules such as IL-1β have been implicated in initiating a cascade of events leading to the activation of PI-3 kinase and fibroblast growth factor 2.[49–52] To date, medium optimization, addition of growth factors and optimization of growth substrates have increased cell yields of HCEC cultures, but may not prevent fibroblastic transformation. Given the loss of function of fibroblastic HCECs, the ability to identify and select functional canonical cells in a mixed culture is critical. Our data confirms in canonical cultures the expression of ZO-1 and Na^+/K^+/ATPase, typical markers of the endothelial monolayer.[53,54] However, these markers are expressed by canonical HCECs only while confluent and forming tight junctions, and their expression decreases once the cells are removed from a monolayer.

This underlines the necessity for identifying other markers for canonical HCECs in suspension. To pursue this, we used microarray analysis of corneal epithelial, stromal, and endothelial tissue, as well as in vitro cultured HCECs to isolate candidate surface markers present either exclusively in the stroma, or in both the native endothelium and the in vitro cultured HCECs. We further tested the expression levels of nine of these candidate markers by flow cytometry in canonical, mixed, and fibroblastic in vitro cultured HCECs. We found four surface-expressed proteins that differ significantly between canonical and fibroblastic HCECs.

CD56, or neural cell adhesion molecule (NCAM), is a surface glycoprotein that exists in multiple isoforms[55–57] and is expressed by multiple cell types.[58–61] It plays an important role in cell adhesion and cell interactions,[62,63] migration,[64] and embryogenesis.[65] Neural cell adhesion molecule expression has been demonstrated in the embryonic chick cornea,[66] with decrease in expression and localization toward the posterior regions of the cornea after birth. Neural cell adhesion molecule has also been localized to the mouse retina[67] and human adult corneal endothelium,[68] consistent with HCECs' embryologic origin from neural crest cells.[69] Neural cell adhesion molecule is expressed by HCECs produced in vitro, however, as the cells undergo EnMT, its expression decreases. Importantly, we found that CD56 expression in cultures also correlated with higher functional barrier capacity in TEER assays. CD248, or endosialin, belongs to the family of C-type lectin transmembrane receptors that may play a role in cell–cell adhesion, host defense, and tumor neoangiogenesis,[70–73] but their role in HCEC biology is unknown. A third canonical marker identified here, Coxsackie adenovirus receptor (CAR), is part of the junctional adhesion molecules (JAMs) family known to participate in a variety of cellular processes, such as leukocyte-platelet-vascular endothelium interactions,[74,75] and tight-junction formation in epithelial and endothelial cells.[76–78] The presence of CAR in the corneal endothelium was previously described,[79] but its biological significance remains unknown. Finally, CD109, a cell surface antigen involved in the TGF-β pathway,[80] has been studied in white blood cells, vascular endothelial cells,[81] keratinocytes,[82] and activated platelets.[83] Its expression increases in some malignancies,[84] an interesting observation consistent with our data demonstrating increased expression as HCECs undergo EnMT. For all of these new markers, further investigation is necessary to explain underlying mechanisms leading to these expression shifts.

Other potential candidates have been identified from microarray analyses and tested via flow cytometry to differentiate canonical HCECs from HCECs undergoing EnMT, including CD166 (ALCAM), expressed in corneal epithelial limbal stem cells[85] but also in corneal stromal stem cells,[86] CD90,[87] expressed in corneal stromal fibroblasts, but also in canonical corneal endothelial cells, and CD73 and CD9.[43] For these last two, no difference between corneal layers was detected by microarray, and further testing by flow cytometry remained negative in our experiments. Given our testing of both gene and protein expression, and use of exclusively human corneal tissue and primary corneal endothelial cells, these data raise questions as to whether CD9 and CD73 will be useful markers to differentiate canonical from fibroblastic HCECs.

Together, the specific surface markers identified here and their correlation to cell function represent a novel set of criteria for the selection of in vitro expanded HCECs that we would hypothesize are most likely to be functionally competent to replace damaged corneal endothelial cells, and thus represent a step toward HCEC therapy. Along with HCEC culture and cell characterization, effort directed toward delivering in vitro cultured HCECs to the patient's endothelial surface is focused on injectable cell therapies,[28,88–90] and transplantable corneal scaffolds.[91–97] Ongoing efforts should demonstrate the feasibility of HCEC in vitro expansion, selection of cultured HCECs with highest function, and development of cell delivery approaches. Recent animal studies using corneal endothelial cells revealed that the cells integrate in vivo to the host endothelium, and are able to restore corneal transparency after injury,[28,98] but many questions such as dosage and stability remain unanswered. Our donor tissue selection criteria, together with the exhaustive characterization provided in this study, are essential for obtaining high quality, functional cultured HCECs, bringing us a step closer to the clinic with a human corneal endothelial cell therapy.

Acknowledgments

The authors thank Cheryl Kim (La Jolla Institute of Allergy and Immunology) and Jonathan Van Dyke and Katarzyna Wilczek (University of California Davis) for assistance with flow cytometry.

Supported by grants from National Eye Institute (P30-EY014801 and P30-EY022125; Bethesda, MD, USA), and an unrestricted grant from Research to Prevent Blindness, Inc. (New York, NY, USA).

Disclosure: **A. Bartakova**, None; **K. Alvarez-Delfin**, None; **A.D. Weisman**, None; **E. Salero**, None; **G.A. Raffa**, None; **R.M. Merkhofer Jr**, None; **N.J. Kunzevitzky**, Emmecell (E), P; **J.L. Goldberg**, Emmecell (S), P

References

1. Murphy C, Alvarado J, Juster R, Maglio M. Prenatal and postnatal cellularity of the human corneal endothelium. A quantitative histologic study. *Invest Ophthalmol Vis Sci*. 1984; 25:312–322.
2. Joyce NC, Harris DL, Mello DM. Mechanisms of mitotic inhibition in corneal endothelium: contact inhibition and TGF-beta2. *Invest Ophthalmol Vis Sci*. 2002;43:2152–2159.
3. Bahn CF, Glassman RM, MacCallum DK, et al. Postnatal development of corneal endothelium. *Invest Ophthalmol Vis Sci*. 1986;27:44–51.
4. Bourne WM, Nelson LR, Hodge DO. Central corneal endothelial cell changes over a ten-year period. *Invest Ophthalmol Vis Sci*. 1997;38:779–782.
5. Gipson IK. Age-related changes and diseases of the ocular surface and cornea. *Invest Ophthalmol Vis Sci*. 2013;54: ORSF48–ORSF53.
6. Bourne WM, Brubaker RF. Use of air to decrease endothelial cell loss during intraocular lens implantation. *Arch Ophthalmol*. 1979;97:1473–1475.

7. Ing JJ, Ing HH, Nelson LR, Hodge DO, Bourne WM. Ten-year postoperative results of penetrating keratoplasty. *Ophthalmology*. 1998;105:1855–1865.
8. Garcia-Pous M, Udaondo P, Garcia-Delpech S, Salom D, Díaz-Llopis M. Acute endothelial failure after cosmetic iris implants (NewIris®). *Clin Ophthalmol*. 2011;5:721–723.
9. Afshari NA, Pittard AB, Siddiqui A, Klintworth GK. Clinical study of Fuchs corneal endothelial dystrophy leading to penetrating keratoplasty - a 30-year experience. *Arch Ophthalmol*. 2006;124:777–780.
10. Schmedt T, Silva MM, Ziaei A, Jurkunas U. Molecular bases of corneal endothelial dystrophies. *Exp Eye Res*. 2012;95:24–34.
11. Vincent AL. Corneal dystrophies and genetics in the International Committee for Classification of Corneal Dystrophies era: a review. *Clin Exp Ophthalmol*. 2013;42:4–12.
12. McLaren JW, Bachman LA, Kane KM, Patel SV. Objective assessment of the corneal endothelium in Fuchs' endothelial dystrophy. *Invest Ophthalmol Vis Sci*. 2014;55:1184–1190.
13. Pascolini D, Mariotti SP. Global estimates of visual impairment: 2010. *Br J Ophthalmol*. 2012;96:614–618.
14. Stevens GA, White RA, Flaxman SR, et al. Global prevalence of vision impairment and blindness: magnitude and temporal trends, 1990-2010. *Ophthalmology*. 2013;120:2377–2384.
15. Bourne RRA, Stevens GA, White RA, et al. Causes of vision loss worldwide, 1990–2010: a systematicanalysis. *Lancet Glob Health*. 2013;1:e339–e349.
16. Melles G, Wijdh R, Nieuwendaal CP. A technique to excise the Descemet membrane from a recipient cornea (descemetorhexis). *Cornea*. 2004;23:286–288.
17. Melles GRJ, Ong TS, Ververs B, van der Wees J. Descemet membrane endothelial keratoplasty (DMEK). *Cornea*. 2006; 25:987–990.
18. Lam FC, Bruinsma M, Melles GRJ. Descemet membrane endothelial transfer. *Curr Opin Ophthalmol*. 2014;25:353–357.
19. Dirisamer M, Yeh RY, van Dijk K, Ham L, Dapena I, Melles GRJ. Recipient endothelium may relate to corneal clearance in Descemet membrane endothelial transfer. *Am J Ophthalmol*. 2012;154:290–296.e291.
20. Chaurasia S, Price MO, McKee Y, Price FWJ. Descemet membrane endothelial keratoplasty combined with epithelial debridement and mitomycin-c application for Fuchs dystrophy with preoperative subepithelial fibrosis or anterior basement membrane dystrophy. *Cornea*. 2014;33:335–339.
21. Price MO, Price FW Jr. Endothelial keratoplasty - a review. *Clin Exp Ophthalmol*. 2010;38:128–140.
22. Anshu A, Price MO, Price FW. Risk of corneal transplant rejection significantly reduced with Descemet's membrane endothelial keratoplasty. *Ophthalmology*. 2012;119:536–540.
23. Feng MT, Price MO, Miller JM, et al. Air reinjection and endothelial cell density in Descemet membrane endothelial keratoplasty: five-year follow-up. *J Cataract Refract Surg*. 2014;40:1116–1121.
24. Burkhardt B. 2013 eye banking statistical report. *EBAA*. 2014;1–114.
25. Okumura N, Koizumi N, Kay EP, et al. The ROCK inhibitor eye drop accelerates corneal endothelium wound healing. *Invest Ophthalmol Vis Sci*. 2013;54:2493–2502.
26. Okumura N, Koizumi N, Ueno M, et al. Enhancement of corneal endothelium wound healing by Rho-associated kinase (ROCK) inhibitor eye drops. *Br J Ophthalmol*. 2011;95:1006–1009.
27. Okumura N, Koizumi N, Ueno M, et al. The new therapeutic concept of using a rho kinase inhibitor for the treatment of corneal endothelial dysfunction. *Cornea*. 2011;30:S54–S59.
28. Koizumi N, Okumura N, Kinoshita S. Development of new therapeutic modalities for corneal endothelial disease focused on the proliferation of corneal endothelial cells using animal models. *Exp Eye Res*. 2012;95:60–67.
29. Joyce NC, Zhu CC. Human corneal endothelial cell proliferation: potential for use in regenerative medicine. *Cornea*. 2004;23(suppl 8):S8–S19.
30. Okumura N, Koizumi N, Ueno M, et al. ROCK inhibitor converts corneal endothelial cells into a phenotype capable of regenerating in vivo endothelial tissue. *Am J Pathol*. 2012;181:268–277.
31. Okumura N, Kay EP, Nakahara M, Hamuro J, Kinoshita S, Koizumi N. Inhibition of TGF-β signaling enables human corneal endothelial cell expansion in vitro for use in regenerative medicine. *PLoS One*. 2013;8:e58000.
32. Okumura N, Nakano S, Kay EP, et al. Involvement of cyclin D and p27 in cell proliferation mediated by ROCK inhibitors Y-27632 and Y-39983 during corneal endothelium wound healing. *Invest Ophthalmol Vis Sci*. 2014;55:318.
33. Okumura N, Nakamura T, Kay EP, Nakahara M, Kinoshita S, Koizumi N. R-spondin1 regulates cell proliferation of corneal endothelial cells via the Wnt3a/beta-catenin pathway. *Invest Ophthalmol Vis Sci*. 2014;55:6861–6869.
34. Zhu C, Joyce NC. Proliferative response of corneal endothelial cells from young and older donors. *Invest Ophthalmol Vis Sci*. 2004;45:1743–1751.
35. Peh GSL, Beuerman RW, Colman A, Tan DT, Mehta JS. Human corneal endothelial cell expansion for corneal endothelium transplantation: an overview. *Transplantation*. 2011;91:811–819.
36. Moysidis SN, Alvarez-Delfin K, Peschansky VJ, et al. Magnetic field-guided cell delivery with nanoparticle-loaded human corneal endothelial cells. *Nanomedicine*. 2015;11:499–509.
37. Stramer BM, Kwok MGK, Farthing-Nayak PJ, Jung J-C, Fini ME, Nayak RC. Monoclonal antibody (3G5)–defined ganglioside: cell surface marker of corneal keratocytes. *Invest Ophthalmol Vis Sci*. 2004;45:807–806.
38. Chakravarti S, Wu F, Vij N, Roberts L, Joyce S. Microarray studies reveal macrophage-like function of stromal keratocytes in the cornea. *Invest Ophthalmol Vis Sci*. 2004;45:3475–3484.
39. Peh GSL, Toh K-P, Wu F-Y, Tan DT, Mehta JS. Cultivation of human corneal endothelial cells isolated from paired donor corneas. *PLoS One*. 2011;6:e28310.
40. Ban Y, Cooper LJ, Fullwood NJ, et al. Comparison of ultrastructure, tight junction-related protein expression and barrier function of human corneal epithelial cells cultivated on amniotic membrane with and without air-lifting. *Exp Eye Res*. 2003;76:735–743.
41. Singh JS, Haroldson TA, Patel SP. Characteristics of the low density corneal endothelial monolayer. *Exp Eye Res*. 2013;115: 239–245.
42. Petroll WM, Hsu JK, Bean J, Cavanagh HD, Jester JV. The spatial organization of apical junctional complex-associated proteins in feline and human corneal endothelium. *Curr Eye Res*. 1999; 18:10–19.
43. Okumura N, Hirano H, Numata R, et al. Cell surface markers of functional phenotypic corneal endothelial cells. *Invest Ophthalmol Vis Sci*. 2014;55:7610–7618.
44. Ding V, Chin A, Peh G, Mehta JS, Choo A. Generation of novel monoclonal antibodies for the enrichment and characterization of human corneal endothelial cells (hCENC) necessary for the treatment of corneal endothelial blindness. *mAbs*. 2014;6: 1439–1452.
45. Bartakova A, Kunzevitzky NJ, Goldberg JL. Regenerative cell therapy for corneal endothelium. *Curr Ophthalmol Rep*. 2014;2:81–90.
46. Nakano Y, Oyamada M, Dai P, Nakagami T, Kinoshita S, Takamatsu T. Connexin43 knockdown accelerates wound healing but inhibits mesenchymal transition after corneal

Investigative Ophthalmology & Visual Science

endothelial injury in vivo. *Invest Ophthalmol Vis Sci*. 2008;49:93–104.

47. Konomi K, Zhu C, Harris D, Joyce NC. Comparison of the proliferative capacity of human corneal endothelial cells from the central and peripheral areas. *Invest Ophthalmol Vis Sci*. 2005;46:4086–4091.
48. Lee JG, Kay EP. FGF-2-mediated signal transduction during endothelial mesenchymal transformation in corneal endothelial cells. *Exp Eye Res*. 2006;83:1309–1316.
49. Lee JG, Ko MK, Kay EP. Endothelial mesenchymal transformation mediated by IL-1β FGF-2 in corneal endothelial cells. *Exp Eye Res*. 2012;95:35–39.
50. Lee JG, Kay EP. NF-kB is the transcription factor for FGF-2 that causes endothelial mesenchymal transformation in cornea. *Invest Ophthalmol Vis Sci*. 2012;53:1530–1538.
51. Lee JG, Heur M. Interleukin-1β enhances cell migration through AP-1 and NF-κB pathway-dependent FGF2 expression in human corneal endothelial cells. *Biol Cell*. 2013;105:175–189.
52. Lee JG, Heur M. Interleukin-1-induced Wnt5a enhances human corneal endothelial cell migration through regulation of Cdc42 and RhoA. *Mol Cell Biol*. 2014;34:3535–3545.
53. Stiemke MM, McCartney MD, Cantu-Crouch D, Edelhauser HF. Maturation of the corneal endothelial tight junction. *Invest Ophthalmol Vis Sci*. 1991;32:2757–2765.
54. Yee RW, Geroski DH, Matsuda M, Champeau EJ, Meyer LA, Edelhauser HF. Correlation of corneal endothelial pump site density, barrier function, and morphology in wound repair. *Invest Ophthalmol Vis Sci*. 1985;26:1191–1201.
55. Cunningham BA, Hemperly JJ, Murray BA, Prediger EA, Brackenbury R, Edelman GM. Neural cell adhesion molecule: structure, immunoglobulin-like domains, cell surface modulation, and alternative RNA splicing. *Science*. 1987;236:799–806.
56. Dickson G, Barton CH, Elsom VL, et al. Alternative splicing generates a secreted form of N-CAM in muscle and brain. *Cell*. 1988;55:955–964.
57. Santoni MJ, Barthels D, Vopper G, Boned A, Goridis C, Wille W. Differential exon usage involving an unusual splicing mechanism generates at least eight types of NCAM cDNA in mouse brain. *EMBO J*. 1989;8:385–392.
58. Lanier LL, Chang C, Azuma M, Ruitenberg JJ, Hemperly JJ, Phillips JH. Molecular and functional analysis of human natural killer cell-associated neural cell adhesion molecule (N-CAM/CD56). *J Immunol*. 1991;146:4421–4426.
59. Dickson G, Gower HJ, Barton CH, et al. Human muscle neural cell adhesion molecule (N-CAM): identification of a muscle-specific sequence in the extracellular domain. *Cell*. 1987;50:1119–1130.
60. Nitta T, Yagita H, Sato K, Okumura K. Involvement of CD56 (NKH-1/Leu-19 antigen) as an adhesion molecule in natural killer-target cell interaction. *J Exp Med*. 1989;170:1757–1761.
61. Cole GJ, Loewy A, Glaser L. Neuronal cell-cell adhesion depends on interactions of N-CAM with heparin-like molecules. *Nature*. 1986;320:445–447.
62. Cole GJ, Schachner M. Localization of the L2 monoclonal antibody binding site on chicken neural cell adhesion molecule (NCAM) and evidence for its role in NCAM-mediated cell adhesion. *Neurosci Lett*. 1987;78:227–232.
63. Kadmon G, Kowitz A, Altevogt P, Schachner M. The neural cell adhesion molecule N-CAM enhances L1-dependent cell-cell interactions. *J Cell Biol*. 1990;110:193–208.
64. Prag S, Lepekhin EA, Kolkova K, et al. NCAM regulates cell motility. *J Cell Sci*. 2002;115(pt 2):283–292.
65. Rutishauser U. Developmental biology of a neural cell adhesion molecule. *Nature*. 1984;310:549–554.
66. Mao X, Schwend T, Conrad GW. Expression and localization of neural cell adhesion molecule and polysialic acid during chick corneal development. *Invest Ophthalmol Vis Sci*. 2012;53:1234–1243.
67. Håkansson J, Ståhlberg A, Wolfhagen Sand F, Gerhardt H, Semb H. N-CAM exhibits a regulatory function in pathological angiogenesis in oxygen induced retinopathy. *PLoS One*. 2011;6:e26026.
68. Foets BJ, van den Oord JJ, Volpes R, Missotten L. In situ immunohistochemical analysis of cell adhesion molecules on human corneal endothelial cells. *Br J Ophthalmol*. 1992;76:205–209.
69. Lwigale PY, Bronner-Fraser M. Semaphorin3A/neuropilin-1 signaling acts as a molecular switch regulating neural crest migration during cornea development. *Dev Biol*. 2009;336:257–265.
70. St. Croix B, Rago C, Velculescu V, Traverso G. Genes expressed in human tumor endothelium. *Science*. 2000;289:1197–1202.
71. Christian S, Ahorn H, Koehler A, et al. Molecular cloning and characterization of endosialin, a C-type lectin-like cell surface receptor of tumor endothelium. *J Biol Chem*. 2001;276:7408–7414.
72. Rupp C, Dolznig H, Puri C, et al. Mouse endosialin, a C-type lectin-like cell surface receptor: expression during embryonic development and induction in experimental cancer neoangiogenesis. *Cancer Immun*. 2006;6:10.
73. Rupp C, Dolznig H, Puri C, et al. Laser capture microdissection of epithelial cancers guided by antibodies against fibroblast activation protein and endosialin. *Diagn Mol Pathol*. 2006;15:35–42.
74. Williams LA, Martin-Padura I, Dejana E, Hogg N, Simmons DL. Identification and characterisation of human junctional adhesion molecule (JAM). *Mol Immunol*. 1999;36:1175–1188.
75. Martin-Padura I, Lostaglio S, Schneemann M, et al. Junctional adhesion molecule, a novel member of the immunoglobulin superfamily that distributes at intercellular junctions and modulates monocyte transmigration. *J Cell Biol*. 1998;142:117–127.
76. Liu Y, Nusrat A, Schnell FJ, et al. Human junction adhesion molecule regulates tight junction resealing in epithelia. *J Cell Sci*. 2000;113:2363–2374.
77. Liang TW, Demarco RA, Mrsny RJ, et al. Characterization of huJAM: evidence for involvement in cell-cell contact and tight junction regulation. *Am J Physiol, Cell Physiol*. 2000;279:C1733–C1743.
78. Mandell K, Parkos C. The JAM family of proteins. *Adv Drug Delivery Rev*. 2005;57:857–867.
79. Mandell KJ, Holley GP, Parkos CA, Edelhauser HF. Antibody blockade of junctional adhesion molecule-A in rabbit corneal endothelial tight junctions produces corneal swelling. *Invest Ophthalmol Vis Sci*. 2006;47:2408–2416.
80. Bizet AA, Tran-Khanh N, Saksena A, Liu K, Buschmann MD, Philip A. CD109-mediated degradation of TGF-β receptors and inhibition of TGF-β responses involve regulation of SMAD7 and Smurf2 localization and function. *J Cell Biochem*. 2011;113:238–246.
81. Hwang SM, Kim MJ, Chang HE, et al. Human platelet antigen genotyping and expression of CD109 (human platelet antigen 15) mRNA in various human cell types. *Biomed Res Int*. 2013;2013:1–5.
82. Finnson KW. Identification of CD109 as part of the TGF-receptor system in human keratinocytes. *FASEB J*. 2006;20:1525–1527.
83. Landau M, Rosenberg N. Molecular insight into human platelet antigens: structural and evolutionary conservation analyses offer new perspective to immunogenic disorders. *Transfusion*. 2010;51:558–569.

Investigative Ophthalmology & Visual Science

84. Hashimoto M, Ichihara M, Watanabe T, et al. Expression of CD109 in human cancer. *Oncogene*. 2004;23:3716–3720.
85. Albert R, Veréb Z, Csomós K, et al. Cultivation and characterization of cornea limbal epithelial stem cells on lens capsule in animal material-free medium. *PLoS One*. 2012;7: e47187.
86. Pinnamaneni N, Funderburgh JL. Concise review: stem cells in the corneal stroma. *Stem Cells*. 2012;30:1059–1063.
87. Pei Y, Sherry DM, McDermott AM. Thy-1 distinguishes human corneal fibroblasts and myofibroblasts from keratocytes. *Exp Eye Res*. 2004;79:705–712.
88. Mimura T, Shimomura N, Usui T, et al. Magnetic attraction of iron-endocytosed corneal endothelial cells to Descemet's membrane. *Exp Eye Res*. 2003;76:745–751.
89. Mimura T, Yamagami S, Usui T, et al. Long-term outcome of iron-endocytosing cultured corneal endothelial cell transplantation with magnetic attraction. *Exp Eye Res*. 2005;80:149–157.
90. Patel SV, Bachman LA, Hann CR, Bahler CK, Fautsch MP. Human corneal endothelial cell transplantation in a human ex vivo model. *Invest Ophthalmol Vis Sci*. 2009;50:2123–2131.
91. Koizumi N, Sakamoto Y, Okumura N, et al. Cultivated corneal endothelial cell sheet transplantation in a primate model. *Invest Ophthalmol Vis Sci*. 2007;48:4519–4526.
92. Blake DA, Yu H, Young DL, Caldwell DR. Matrix stimulates the proliferation of human corneal endothelial cells in culture. *Invest Ophthalmol Vis Sci*. 1997;38:1119–1129.
93. Griffith M. Functional human corneal equivalents constructed from cell lines. *Science*. 1999;286:2169–2172.
94. Takezawa T, Ozaki K, Nitani A, Takabayashi C, Shimo-Oka T. Collagen vitrigel: a novel scaffold that can facilitate a three-dimensional culture for reconstructing organoids. *Cell Transplant*. 2004;13:463–473.
95. Fagerholm P, Lagali NS, Merrett K, et al. A biosynthetic alternative to human donor tissue for inducing corneal regeneration: 24-month follow-up of a phase 1 clinical study. *Science*. 2010;2:46ra61.
96. Karamichos D, Funderburgh ML, Hutcheon AEK, et al. A Role for topographic cues in the organization of collagenous matrix by corneal fibroblasts and stem cells. *PLoS One*. 2014;9: e86260.
97. Karamichos D, Hutcheon AEK, Zieske JD. Transforming growth factor-β3 regulates assembly of a non-fibrotic matrix in a 3D corneal model. *J Tissue Eng Regen Med*. 2011;5:e228–e238.
98. Koizumi N, Sakamoto Y, Okumura N, et al. Cultivated corneal endothelial transplantation in a primate: possible future clinical application in corneal endothelial regenerative medicine. *Cornea*. 2008;27(suppl 1):S48–S55.

Investigative Ophthalmology & Visual Science